Evidence for the Lack of a Specific Interaction between Cholesterol and Sphingomyelin

Juha M. Holopainen,*† Antti J. Metso,* Juha-Pekka Mattila,* Arimatti Jutila,* and Paavo K. J. Kinnunen*‡
*Helsinki Biophysics & Biomembrane Group, Institute of Biomedicine, University of Helsinki, Finland;
†Department of Ophthalmology, University of Helsinki, Finland; and ‡MEMPHYS—Center for Biomembrane Physics, University of Southern Denmark, Odense, Denmark

ABSTRACT The putative specific interaction and complex formation by sphingomyelin and cholesterol was investigated. Accordingly, low contents (1 mol % each) of fluorescently labeled derivatives of these lipids, namely 1-palmitoyl-2[10-(pyren-1-yl)]decanoyl-*sn*-glycero-3-phosphocholine (PyrPC), *n*-[10-(1-pyrenyl)decanoyl]sphingomyelin (PyrSM), and increasing concentrations of cholesterol (up to 5 mol %), were included in large unilamellar vesicles composed of 1,2-dimyristoyl-*sn*-glycero-3-phosphocholine (DMPC) or 1,2-dinervonoyl-*sn*-glycero-3-phosphocholine (DNPC), and the excimer/monomer fluorescence emission ratio (I_e/I_m) was measured. In DNPC below the main phase transition, the addition of up to 5 mol % cholesterol reduced I_e/I_m significantly. Except for this, cholesterol had only a negligible effect in both matrices and for both probes. We then compared the efficiency of resonance energy transfer from PyrPC and PyrSM to 22-(*n*-(7-nitrobenz-2-oxa-1,3-diazol-4-yl)amino)-23,24-bisnor-5-cholen-3β-ol (NBDchol). An augmenting colocalization of the latter resonance energy transfer pair with temperature was observed in a DMPC matrix below the main phase transition. In contrast, compared to PyrSM the colocalization of PyrPC with NBDchol was more efficient in the longer DNPC matrix. These results could be confirmed using 5,6-dibromo-cholestan-3β-ol as a collisional quencher for the pyrene-labeled lipids. The results indicate lack of a specific interaction between sphingomyelin and cholesterol, and further imply that hydrophobic mismatch between the lipid constituents could provide the driving force for the cosegregation of sphingomyelin and cholesterol in fluid phospholipid bilayers of thicknesses comparable to those found for biomembranes.

INTRODUCTION

The lipid bilayer provides the basic structural framework for cellular membranes. These soft interfaces are composed of a vast number of diverse lipid constituents (Kinnunen, 1991) and in terms of physics are thus classified as many body systems possessing order on various time- as well as length scales (Kinnunen, 1991; Jacobson et al., 1995; Glaser, 1995; Mouritsen and Kinnunen, 1996; Varma and Mayor, 1998; Hwang et al., 1998). The physical properties and the thermodynamic state of the bilayer influence the functions and lateral organization of the contained membrane proteins (Mustonen et al., 1987; Hønger et al., 1997; Vaz and Almeida, 1993), whereas proteins also determine, in part, the ordering of the lipids in bilayer (Mouritsen and Bloom, 1984; Asturias et al., 1990; Lehtonen and Kinnunen, 1997). The molecular mechanisms and processes underlying the dynamic ordering of biomembranes are being intensively investigated (e.g., Mouritsen and Kinnunen, 1996; Mouritsen, 1998).

Recently, sphingomyelin and cholesterol have been suggested to form microdomains (rafts), which then participate to recruit proteins and lipid signaling molecules into these assemblies (Brown and London, 2000). Both cholesterol and sphingomyelin are abundant components of eukaryote membranes (Bretscher and Munro, 1993). These lipids have been shown to colocalize in the same membrane compartments, with >50% of the cellular sphingomyelin and unesterified cholesterol found in the plasma membrane (Kolesnick, 1991). Manipulation of the membrane content of either cholesterol or sphingomyelin results in parallel changes in the rates of synthesis of these two lipids. Accordingly, loading of fibroblast plasma membrane with sphingomyelin results in reduced esterification of intracellular cholesterol and increased cholesterol synthesis leading to higher contents of cholesterol in the plasma membrane (Gatt and Bierman, 1980). Degradation of fibroblast plasma membrane sphingomyelin activates endogenous cholesterol esterification and downregulates the activity of the rate-limiting enzyme of cholesterol synthesis, HMG-CoA reductase (Slotte and Bierman, 1988; Gupta and Rudney, 1991). The capacity of the plasma membrane to solubilize cholesterol appears to depend on the sphingomyelin content (Okwu et al., 1994). Importantly, enzymatic degradation of cellular phosphatidylcholine does not affect cellular cholesterol esterification (Pörn et al., 1993). Furthermore, whereas enzymatic sphingomyelin degradation increases cholesterol efflux to β-cyclodextrin, degradation of phosphatidylcholine has no effect (Ohvo et al., 1997). The physiological significance of the metabolic coupling between cholesterol and sphingomyelin levels remains unknown, in addition to the actual molecular level mechanism(s) coupling the contents of these lipids in membranes.

Complex formation due to a high affinity interaction between sphingomyelin and cholesterol has been suggested. The origin of this hypothesis can be traced to the condensation of sphingomyelin monolayers in the presence of choles-

Submitted May 7, 2003, and accepted for publication October 17, 2003.

Address reprint requests to Paavo K. J. Kinnunen, Institute of Biomedicine/Biochemistry, PO Box 63 (Biomedicum, Haartmaninkatu 8), FIN-00014, University of Helsinki, Helsinki, Finland. Tel.: 358-9-191-25400; Fax: 358-9-191-25444; E-mail: paavo.kinnunen@helsinki.fi.

0006-3495/04/03/1510/11 $2.00

terol (Demel et al., 1977), which has been subsequently confirmed by a number of laboratories (e.g., Lund-Katz et al., 1988; Needham and Nunn, 1990; Mattjus and Slotte, 1996; Ramstedt and Slotte, 1999; Radhakrishnan et al., 2000, 2001; Veiga et al., 2001; Li et al., 2001). In addition, cholesterol efflux from Langmuir films to cyclodextrin added into the aqueous subphase has been shown to decrease when the sphingomyelin/phosphatidylcholine ratio is increased (reviewed in Slotte, 1999). This finding has been taken as evidence suggesting sphingomyelin to have higher affinity to cholesterol than to the corresponding phosphatidylcholine. Subsequent studies in other laboratories using this technique suggest that sphingomyelin and cholesterol form condensed complexes with a stoichiometry of ~2:1 (Radhakrishnan et al., 2000, 2001; Li et al., 2001). However, phosphatidylcholines also form condensed complexes with cholesterol (Smaby et al., 1994, 1997; Keller et al., 2000). Importantly, conclusive evidence demonstrating lack of specific sphingomyelin-cholesterol interaction has been presented (Untracht and Shipley, 1977; Calhoun and Shipley, 1979; Lange et al., 1979; Schroeder and Nemecz, 1989; Smaby et al., 1994; Mannock et al., 2003).

Sphingomyelin is composed of a polar phosphatidylcholine headgroup, a long chain (typically 18 carbon atoms) sphingoid base, and an amide-linked acyl chain. Typically, the acyl chains are long (16–24 carbon atoms) and saturated (Curatolo, 1987). These lipids typically have high chain melting temperatures, exceeding the body temperature of 37°C (Estep et al., 1979). Compared to common unsaturated phosphatidylcholines, saturated fatty acids of the sphingoid base should favor van der Waals interactions with the rigid and planar tetracyclic ring system of cholesterol (McIntosh et al., 1992). Both hydrogen-bond donating and accepting groups are found in the interfacial region of sphingomyelin (Boggs, 1987), in distinction from phosphoglycerides (such as phosphatidylcholine) with two hydrogen-bond accepting carbonyl groups (Brown, 1998). The 3β-OH-group of cholesterol, which is positioned toward the aqueous interface, has been suggested to hydrogen-bond to the carbonyl group of the amide group of sphingomyelin (Sankaram and Thompson, 1990; Bittman et al., 1994). Recent NMR study, however, reveals lack of hydrogen-bonding between sphingomyelin and cholesterol (Guo et al., 2002).

In this study we have addressed the putative interaction between cholesterol and sphingomyelin. Most of the previous studies on this interaction have used large contents of sphingomyelin and/or cholesterol (e.g., Mattjus and Slotte, 1996; Needham and Nunn, 1990; Sankaram and Thompson, 1991;) Ramstedt and Slotte, 1999; Radhakrishnan et al., 2000, 2001; Veiga et al., 2001; Li et al., 2001), which might obscure possible specific interaction. Accordingly, we compared the impact of cholesterol on pyrene-labeled sphingomyelin and phosphatidylcholine derivatives at low concentrations in neutral phosphatidylcholine matrices. In addition, we also compared the efficiency of resonance energy transfer (RET) between trace amounts (mol fraction, $X = 0.01$) of either pyrene-labeled sphingomyelin (PyrSM) or phosphatidylcholine (PyrPC) and NBD-labeled cholesterol. Furthermore, the efficiency of collisional quenching of PyrSM and PyrPC by 5,6-dibromo-cholestan-3β-ol was studied. Both dimyristoylphosphatidylcholine (DMPC) and dinervonoylphosphatidylcholine (DNPC) were compared as matrices to investigate the possible impact of hydrophobic mismatch on the distribution of the fluorescent lipid analogs and cholesterol and its derivatives. The impact of the included fluorescent tracers on the main phase transition of the matrix phospholipids was studied by differential scanning calorimetry (DSC). In summary, we find no evidence for a specific interaction between sphingomyelin and cholesterol, and postulate that the driving force for the colocalization of cholesterol and sphingomyelin in biomembranes is provided by the hydrophobic matching condition.

MATERIALS AND METHODS

Materials

Cholesterol, DNPC, PyrSM, HEPES, and EDTA were obtained from Sigma (St. Louis, MO) and DMPC from Princeton Lipids (Princeton, NJ). PyrPC was from K&V Bioware (Espoo, Finland) and 22-(*n*-(7-nitrobenz-2-oxa-1,3-diazol-4-yl)amino)-23,24-bisnor-5-cholen-3β-ol (NBDchol) from Molecular Probes (Eugene, OR). No impurities were detected in the above lipids upon thin-layer chromatography on silicic acid-coated plates using chloroform/methanol/water/ammonia (65:20:2:2, by volume) as the solvent system and examination of the plates for pyrene or NBD fluorescence under ultraviolet illumination or after iodine staining. The concentrations of DMPC, DNPC, and cholesterol were determined gravimetrically (Cahn, Cerritos, CA). Concentrations of the fluorescent lipids were determined by measuring absorbance at 342 nm and using 42,000 cm^{-1} as the molar extinction coefficient for PyrPC and PyrSM. For NBDchol, 22,000 cm^{-1} at 465 nm was employed. Water was freshly deionized in a Milli RO/Milli Q (Millipore, Billerica, MA) filtering system.

Synthesis of 5,6-dibromo-cholestan-3β-ol

Cholesterol was converted into 5,6-dibromo-cholestan-3β-ol (diBrChol) by reacting with bromide in acetic acid (Streitwieser and Heathcock, 1985). More specifically, cholesterol (1.0 g) was added to a solution of bromide (0.5 g) dissolved in acetic acid (5.0 ml). The reaction mixture was then left for 30 min at room temperature. The separated solid diBrChol was filtered and rinsed with acetic acid (5.0 ml) and purified water. Subsequently, the product was dried. Recrystallization from acetone gave pure product (melting point 110–112°C), which revealed a single spot upon thin layer chromatography performed as above.

Preparation of liposomes

Samples were prepared by dissolving and mixing the indicated lipids in chloroform to obtain the desired compositions, whereafter the solvent was removed under a stream of nitrogen. The residues were subsequently maintained under reduced pressure for >2 h and then hydrated in 20 mM HEPES and 0.1 mM EDTA buffer at pH 7.0 at 65°C (i.e., exceeding the main phase transition temperature of the matrix lipid) to yield a lipid concentration of one mM. The hydrated lipid mixtures were subsequently extruded with a LiposoFast small-volume homogenizer (Avestin, Ottawa,

Canada) to obtain large unilamellar vesicles (LUVs) by subjecting the lipid dispersions to 19 passes through a polycarbonate filter (100-nm pore size, Nucleopore, Pleasanton, CA). All samples were annealed by taking them five times through the transition by repeated heating and cooling between 0 and 37°C, whereafter they were stored at 4°C overnight.

Fluorescence spectroscopy

Fluorescence measurements were carried out with a PerkinElmer LS50B (Wellesley, MA) or a Cary Eclipse (Varian Instruments, Walnut Creek, CA) spectrofluorometer interfaced to a personal computer. Cuvette temperature was controlled by a circulating water bath, and the contents were continuously agitated by a magnetic stirring bar. Pyrene-labeled lipids were excited at 344 nm, and monomer and excimer emission intensities were detected at 398 and 480 nm, respectively, with bandpasses of 4.0 nm. Due to the low concentrations of the chromophores used, inner filter effect can be expected to be negligible. When indicated, the two fluorescent probes, PyrPC and PyrSM, were used as donors and NBDchol as RET acceptor in LUVs (Jutila and Kinnunen, 1997).

Collisional quenching of pyrene excimer emission

Heavy atoms such as iodine and bromine can be used as collisional quenchers for fluorescence due to promoting intersystem crossing to an excited triplet state, promoted by spin-orbit coupling of the excited fluorophore and the halogen (Lakowicz, 1999). Accordingly, we used diBrChol as a collisional quencher for the emission of PyrPC and PyrSM. For both RET and collisional quenching the data are expressed as colocalization parameter C. In brief, the colocalization of these pairs were assessed by defining the colocalization parameter C as

$$C = (I_0 - I)/I_0,$$

where I_0 and I are emission intensities at 480 nm measured for PyrPC/PyrSM in the absence and presence of the acceptor, respectively (Jutila and Kinnunen, 1997). In addition to the excitation peak at 470 nm, NBD has a second, significantly weaker absorption band centered at ~335 nm and accordingly, the latter could contribute to the 480-nm excimer emission from the pyrene-labeled probes. However, this emission was found to be negligible (data not shown). Maximum ($I \rightarrow 0$) for C indicates augmented colocalization of the probes whereas minimum ($I \rightarrow I_0$) reports the probes being dispersed in the membrane. Importantly, quantitative analysis of the resonance energy transfer data is ambiguous due to the lack of information on the orientation of the oscillating dipoles of the fluorophores and uncertainty concerning probe distribution (Drake et al., 1991). This drawback, however, does not compromise the qualitative conclusions of the present study. Furthermore, due to extensive, and compared to the fluorescence lifetimes, very rapid thermal motion of the chromophores, it is highly unlikely that mutual orientation of the oscillating dipoles would limit the efficiency of RET. Accordingly, changes in RET can be readily expected to be mostly determined by changes in the average distances between the donor and acceptor (Jutila and Kinnunen, 1997).

Final concentration of lipid was 25 μM. All temperature scans were performed by increasing the temperature in 0.1–1.1°C steps from 11 to 30°C (DMPC) or from 15 to 37°C (DNPC), the average heating rate being ~0.1°C/min close to the main phase transition of DMPC or DNPC. All experiments were repeated at least once to ensure reproducibility.

Differential scanning calorimetry

Differential heat capacity scans were recorded with a high-sensitivity differential scanning instrument VP-DSC (MicroCal, Northampton, MA) at a lipid concentration of 0.7 mM (heating rate of 0.5°C/min). All experiments were performed in duplicates to ensure reproducibility. The calorimeter was interfaced to a personal computer and data were analyzed using the routines of the Origin software (Microcal, Northampton, MA). We have routinely subjected both multilamellar vesicles (MLVs) as well as extruded vesicles to DSC (Jutila and Kinnunen, 1997; Metso et al., 2003) to check for the loss of material in the extrusion process. Between 25 and 50% of DNPC was found to bind to the filters whereas DMPC appeared to be quantitatively recovered (A. Metso and P. K. J. Kinnunen, unpublished results). Accordingly, because of the uncertainty regarding the actual mass only T_m values are reported for LUVs.

RESULTS

Differential scanning calorimetry

Differential scanning calorimetry was utilized to assess the impact of the fluorescent probes on the thermotropic phase behavior of the studied lipid membranes. DMPC MLVs show upon heating two endotherms corresponding to the pretransition at ~14°C and the main transition at ~23.7°C. In keeping with our previous studies (Jutila and Kinnunen, 1997) LUVs composed of this phospholipid lack the pretransition and exhibit a single endotherm at ~24.1°C (Table 1; see also Jutila and Kinnunen, 1997). The amounts of the probes used (1–2 mol %) in the fluorescence measurements abolished the pretransition peak, broadened the main transition endotherm, and slightly shifted T_m of DMPC MLVs. Likewise, the total enthalpy of the main transition peak was decreased, revealing reduced increment of *trans* → *gauche* isomerization at the transition, which is likely to reflect the chain disordering effect of the probes below T_m (Jutila and Kinnunen, 1997; Metso et al., 2003). DNPC MLVs and LUVs show only the main phase transition endotherm at 26.9 and 26.7°C, respectively. Similarly to DMPC the utilized fluorescent probes broaden the main phase transition endotherm of DNPC and lower the transition temperature (Table 1). Taken together, the above DSC data

TABLE 1 The main transition temperatures (T_m) for large unilamellar vesicles as well as T_m and enthalpies for multilamellar vesicles with the indicated compositions

	T_m, °C		ΔH_m, kJ/mol
	MLVs	LUVs	MLVs
DMPC	23.7	24.1	25.2
PyrPC/DMPC (1:99)	23.6	23.9	22.3
PyrSM/DMPC (1:99)	23.6	23.5	22.5
PyrPC/NBDchol /DMPC (1:1:98)	23.4	23.8	23.2
PyrSM/NBDchol/DMPC (1:1:98)	23.1	23.5	21.1
PyrPC/diBrChol/DMPC (1:1:98)	23.3	23.6	22.9
PyrSM/diBrChol/DMPC (1:1:98)	23.2	23.5	22.9
DNPC	26.9	26.7	69.8
PyrPC/DNPC (1:99)	26.7	26.5	69.9
PyrSM/DNPC (1:99)	26.6	26.2	64.5
PyrPC/NBDchol /DNPC (1:1:98)	26.7	26.1	66.6
PyrSM/NBDchol/DNPC (1:1:98)	64.2	26.5	26.2
PyrPC/diBrChol/DNPC (1:1:98)	26.4	26.0	61.9
PyrSM/diBrChol/DNPC (1:1:98)	26.3	26.7	65.8

Total phospholipid concentration was 0.7 mM in 20 mM HEPES and 0.1 mM EDTA at pH 7.0.

show that in these two types of liposomes (i.e., MLVs versus LUVs), the fluorescent lipid analogs cause only a relatively minor perturbation of the thermotropic behavior of DMPC and DNPC.

The behavior of pyrene-labeled lipids residing in DMPC and DNPC

To study the putative complex formation by sphingomyelin/phosphatidylcholine and cholesterol excimer fluorescence, resonance energy transfer and collisional quenching were utilized to gain insight into the organization of the fluorescent lipid probes below, above, and at T_m, of two neutral phosphatidylcholine matrices, DMPC and DNPC.

DMPC matrix

I_e/I_m for PyrPC residing in DMPC liposomes increases almost linearly upon heating up to ~4.5° below T_m, in keeping with increased lateral diffusion (Hresko et al., 1986; Lehtonen and Kinnunen, 1995). Subsequently, a peak in I_e/I_m becomes evident (denoted by T^* in Fig. 1 *A*), preceding the peak in specific heat at $T_m \sim 24.1$°C determined by DSC. A likely explanation for the pronounced increase in the excimer formation at $T_0 < T < T^*$ for PyrPC in DMPC is lateral enrichment of the probe into the boundary between gel- and fluid-like regions of the membrane (Jutila and Kinnunen, 1997). First derivative $d(I_e/I_m)$ versus $(T–T_m)$ reveals a baseline process progressively enhancing I_e/I_m whereas there is a abrupt increase beginning at ~4.5°C and peaking at ~1.5°C below T_m (Jutila and Kinnunen, 1997). Just below T_m the values for I_e/I_m return close to the ascending baseline attributed to the thermally enhanced excimer formation, increasing I_e/I_m linearly with further increase in temperature. Notably, the slope of the I_e/I_m versus $(T–T_m)$ curve is augmented above T_m compared to the slope below T_m, thus implying that the thermally activated increments in the rate of lateral diffusion in gel and fluid phases are not of similar magnitude.

Compared to PyrPC the I_e/I_m ratio for PyrSM residing in DMPC liposomes is significantly lower (Fig. 1 *A*). The lower efficiency of excimer formation in dipalmitoylphosphatidylcholine matrix by PyrSM compared to PyrPC has been suggested to reflect slower lateral diffusion of the former probe (Somerharju et al., 1985; Hresko et al., 1987). Transition temperature measured for PyrSM is higher than for PyrPC (43 and 15°C, respectively; Somerharju et al., 1985; Hresko et al., 1987). Judged from the enthalpies derived from DSC the disordering effect by PyrPC is more significant than that due to PyrPC. For both probes their phosphocholine headgroup is nearly parallel to the membrane surface. Repulsive potential due to the strongly hydrated headgroups would thus prevent close intermolecular encounters for both PyrPC and PyrSM. It can be anticipated that because of the higher melting temperature of

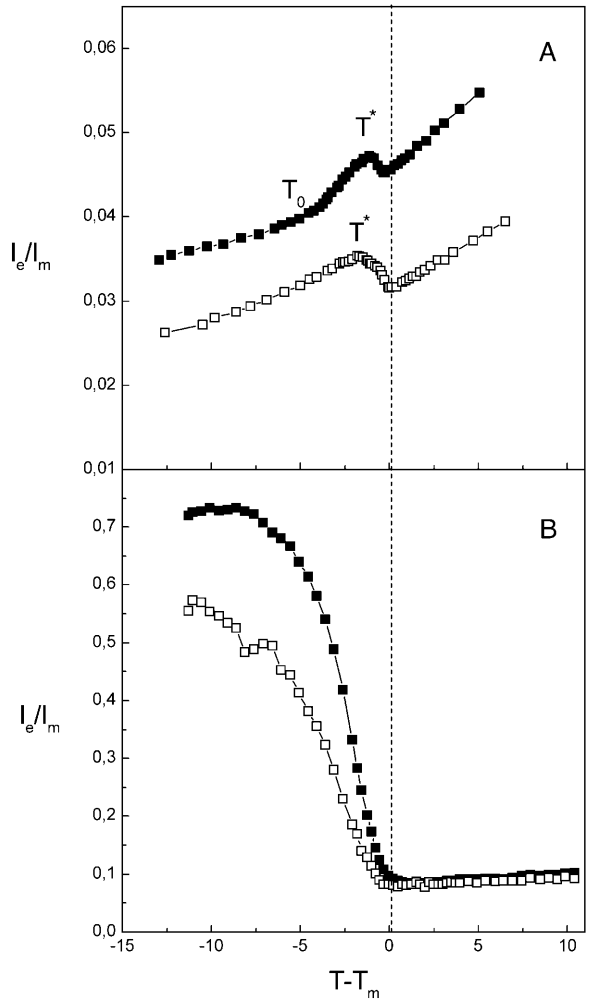

FIGURE 1 (*A*) I_e/I_m versus $T–T_m$ for PyrPC (■) and PyrSM (□) residing in LUVs of DMPC at X_{probe} of 0.01. (*B*) I_e/I_m versus $T–T_m$ for PyrPC (■) and PyrSM (□) residing in DNPC LUVs at $X_{probe} = 0.01$. Total phospholipid concentration was 25 μM in 20 mM HEPES and 0.1 mM EDTA at pH 7.0.

PyrSM the chains of this probe are on the average more ordered than those of PyrPC. Accordingly, the effective length of PyrSM should exceed that of PyrPC and the pyrene moiety of the former probe should therefore interdigitate into the adjacent leaflet more efficiently than PyrPC, thus reducing I_e/I_m. This would be in keeping with the slightly reduced enthalpy observed by DSC (Table 1). Similarly to PyrPC the I_e/I_m values for PyrSM increase monotonically from 0.026 to 0.033 upon heating to ~2° below T_m (~23.5°C). A local minimum is observed at T_m, and is followed by a continuous and approximately linear increase in I_e/I_m. Interestingly, the decrease in I_e/I_m (from T^* to T_m) for PyrSM is less steep and takes place over a wider temperature range than for PyrPC. The absence of the transient peak in I_e/I_m for PyrSM indicates that this probe behaves in a different way in this temperature range, probably being enriched into microdomains and preferring

the gel state domains of DMPC and reflecting the higher transition temperature measured for PyrSM compared to PyrPC (43 and 15°C, respectively). For PyrSM I_e/I_m versus (T–T_m) the slopes below and above T_m are approximately equal. First derivative $d(I_e/I_m)$ versus (T–T_m) shows that the transient peak in I_e/I_m between 4.5 and 1.5° below T_m observed for PyrPC is lacking for PyrSM, and only the baseline process increases I_e/I_m (not shown).

DNPC matrix

Increasing the hydrophobic thickness of the bilayer by substituting DNPC for DMPC causes an increase by one order of magnitude in I_e/I_m for PyrPC when $T < T_m$ (Fig. 1 *B*). Although lateral diffusion of this probe could be higher in DNPC it is also possible that interdigitation and possibly also tilting of chains could reduce I_e/I_m in DMPC. Only modest changes in I_e/I_m for PyrPC are observed below T_m, with the decrement in I_e/I_m for PyrPC beginning at ~6° below T_m. Above T_m there is a slight increase in I_e/I_m.

Similarly to PyrPC also for PyrSM the I_e/I_m values were significantly higher in DNPC. Compared to PyrPC the I_e/I_m values for PyrSM in DNPC are lower below T_m, in keeping with the data on DMPC LUVs, whereas at $T > T_m$ the I_e/I_m ratios are approximately equal for both probes (Fig. 1 *B*). First derivative $d(I_e/I_m)$ versus (T–T_m) revealed the behavior of PyrSM to be almost identical to PyrPC (not shown).

Effect of cholesterol

Subsequent to observing the temperature-dependent changes in I_e/I_m for the two pyrene-labeled lipids, PyrPC and PyrSM in DMPC and DNPC matrices, we investigated the effects of cholesterol on these probes. Increasing the contents of cholesterol (up to 5 mol %) in DMPC LUVs had negligible effect on the I_e/I_m for PyrPC as well as PyrSM both below as well as above T_m (Fig. 2 *A*).

For the thicker DNPC bilayer inclusion of cholesterol caused a pronounced and progressive decrease in I_e/I_m for both PyrPC and PyrSM below T_m (Fig. 2 *B*). However, above T_m no changes in I_e/I_m for either PyrPC or PyrSM were observed.

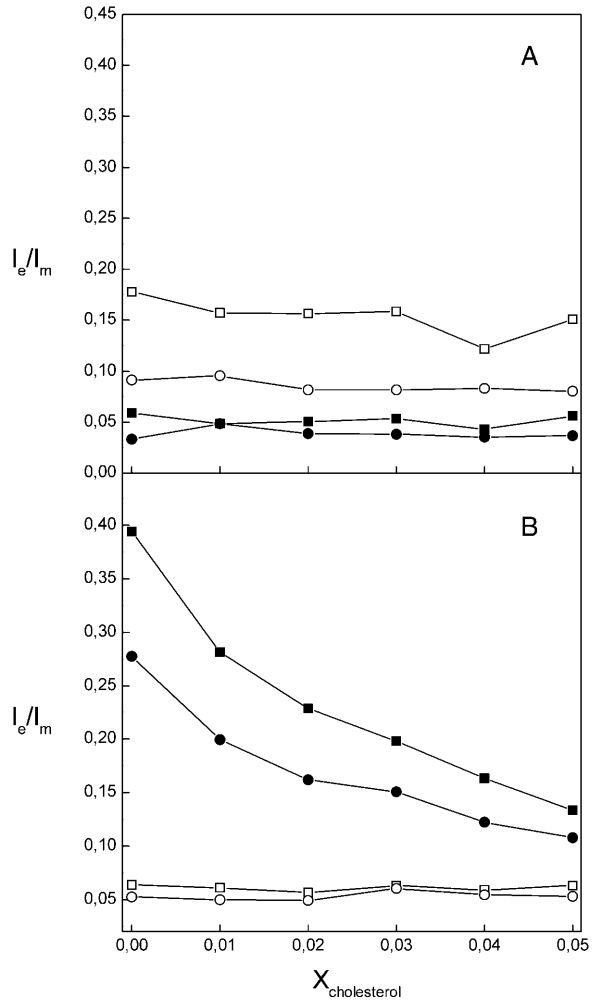

FIGURE 2 I_e/I_m versus increasing contents of cholesterol for PyrPC and PyrSM residing in LUVs of DMPC (*A*) and DNPC (*B*) below (15°C; ■, PyrPC; ●, PyrSM) and above (40°C; □, PyrPC; ○, PyrSM) the main phase transition temperature of the matrix lipid. Total phospholipid concentration was 25 μM in 20 mM HEPES and 0.1 mM EDTA at pH 7.0.

Resonance energy transfer between pyrene-labeled lipids and NBD-cholesterol

Cholesterol has been suggested to reduce line tension between coexisting solid and fluid domains, favoring its partitioning into the interface (Weis and McConnell, 1985; McConnell, 1991; Hwang et al., 1995; Mouritsen et al., 1995). The spectral properties of NBD allow this probe to function as RET acceptor for pyrene. Accordingly, we have previously demonstrated using 22-(*n*-(7-nitrobenz-2-oxa-1,3-diazol-4-yl)amino)-23,24-bisnor-5-cholen-3β-ol (at $X = 0.01$), i.e., a cholesterol analog containing a covalently-linked NBD moiety, that PyrPC and NBDchol become colocalized in the course of the main transition of DMPC (Jutila and Kinnunen, 1997). In this study, we compared two RET pairs—namely, PyrSM with NBDchol and PyrPC with NBDchol.

DMPC matrix

In keeping with our earlier study (Jutila and Kinnunen, 1997) the influence of NBDchol on the temperature dependence of I_e/I_m for PyrPC is dramatic (Fig. 3 *A*). For PyrPC in the presence of NBDchol the values for I_e/I_m increase progressively with temperature, whereas the peak observed at T^* in the absence of the quencher is lacking. The fact that I_e/I_m is increased by NBDchol is likely to reflect efficient quenching of pyrene by this acceptor and colocalization of NBDchol and PyrPC over the whole temperature range

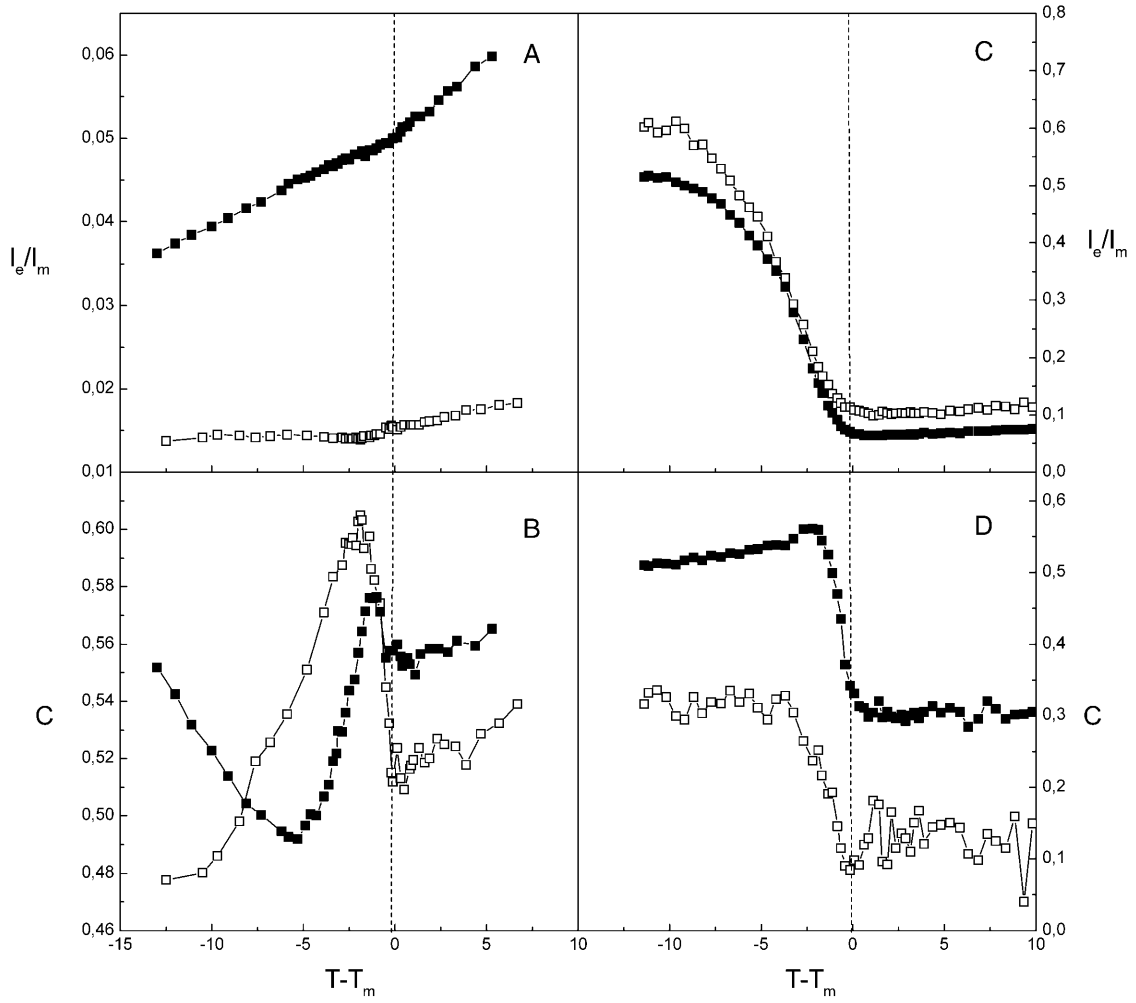

FIGURE 3 Values for I_e/I_m versus T–T_m for DMPC LUVs incorporating PyrPC (■) or PyrSM (□) ($X = 0.01$) together with NBDchol ($X = 0.01$) (*A*) Colocalization parameter *C* versus T–T_m calculated for the respective PyrPC- (■) or PyrSM- (□) NBDchol acceptor pair (*B*). (*C*) Values for I_e/I_m versus T–T_m for DNPC LUVs incorporating PyrPC (■) or PyrSM (□) ($X = 0.01$) together with NBDchol ($X = 0.01$). Colocalization parameter *C* versus T–T_m calculated for the respective PyrPC- (■) or PyrSM- (□) NBDchol acceptor pair residing in DNPC (*D*). The experimental conditions were similar to those described in Fig. 1.

studied, with efficient coupling of the dipoles of excited monomeric PyrPC and NBDchol. *C* versus (T–T_m) reveals colocalization in the gel phase to diminish with first minimum at ~5°C below T_m (Fig. 3 *B*). Thereafter a peak in colocalization is evident at T^*, subsequently followed by a minimum at ~T_m. Upon further increase in temperature above T_m there is a slight increase in *C*. Assuming NBDchol to favor partitioning into the gel-fluid interface similarly to cholesterol, the data strongly suggest the peak in I_e/I_m for PyrPC at T^* to result from a preference of this probe and NBDchol for the domain boundary.

In the presence of NBDchol the I_e/I_m values for PyrSM are significantly lower throughout the temperature range studied (Fig. 3 *A*). There is no increase in I_e/I_m upon increasing the temperature up to 1.5° below T_m whereafter this ratio increases nearly linearly. In contrast to PyrPC/NBDchol, *C* versus (T–T_m) for PyrSM/NBDchol/DMPC mixture reveals efficient colocalization of these probes well below T_m, with no local minima (Fig. 3 *B*). Subsequently, a peak in colocalization at T^* is evident, followed by a minimum at ~T_m. Further increase in temperature induces a slight increase in *C*. Above T_m the lower values for *C* in PyrSM/NBDchol versus PyrPC/NBDchol could result from lower lateral diffusion rate for PyrSM compared to PyrPC. Notably, comparing the absolute values for *C* between different RET pairs is ambiguous, as discussed previously. Yet, our data suggest a pronounced colocalization of PyrSM and NBDchol into the emerging phase boundary between fluid and gel phase domains.

DNPC matrix

The influence of NBDchol on the temperature dependency of I_e/I_m for PyrPC in DNPC matrix was much less dramatic than

in DMPC. In contrast to the results obtained with DMPC, the I_e/I_m ratio throughout the studied temperature range is decreased when NBDchol is present (Fig. 3 *C*). At ~6° below T_m a sudden decrease in I_e/I_m ratio becomes evident, reflecting the gel-to-fluid melting process(es). Interestingly, a high degree of colocalization of PyrPC with NBDchol is evident at all studied temperatures (Fig. 3 *D*), with *C* versus (T–T_m) revealing slightly enhanced colocalization when $T \rightarrow T_m$ with a maximum at ~2° below T_m. Subsequently, a minimum is observed at ~T_m, with further increase in T resulting in a minor increment in *C*.

Throughout the temperature range NBDchol has only a minor effect on the I_e/I_m ratio for PyrSM (Fig. 3 *C*), and *C* versus (T–T_m) for PyrSM/NBDchol reveals much less colocalization for these probes compared to PyrPC/NBDchol (Fig. 3 *D*). No changes in *C* are seen when $T < T_m$. At ~6° below T_m the I_e/I_m ratio begins to rapidly decrease reaching a minimum at T_m. In contrast to DMPC matrix, no enhanced colocalization is observed in the vicinity of T_m and at $T > T_m$ no changes in *C* are observed (Fig. 3 *D*).

Collisional quenching of pyrene excimer emission by 5,6-dibromo-cholestan-3β-ol

Due to its relatively large fluorophore moiety NBDchol can be presumed not to behave identically to cholesterol. Accordingly, to verify the above results with a less perturbing cholesterol analog, we used the collisional quencher 5,6-dibromo-cholestan-3β-ol instead of NBDchol. The brominated derivative lacks the fluorophore moiety and can thus be anticipated to behave more similarly, albeit not identically, to natural cholesterol. The colocalization of PyrSM and PyrPC with diBrChol was compared in DMPC and DNPC matrices by calculating parameter *C* as defined above. Regarding the differences in the resonance energy transfer and collisional quenching data it is important to take into account that RET occurs over considerably longer distances and includes quenching of the donor also in the adjacent leaflet of the bilayer. Instead, collisional quenching requires actual molecular encounters.

DMPC matrix

Except for the values for I_e/I_m being smaller the influence of diBrChol on the temperature dependency of I_e/I_m for PyrPC in DMPC was very similar to that of NBDchol (data not shown). *C* versus (T–T_m) reveals close range colocalization to diminish progressively upon increasing temperature, reaching a local minimum at T_m (Fig. 4 *A*). Above T_m there is a slight increase in *C*.

For PyrSM with diBrChol the values for I_e/I_m were lower than for PyrPC, and only a modest increase in I_e/I_m was observed, similarly to the above results for PyrSM with NBDchol. However, *C* versus (T–T_m) revealed efficient close range colocalization throughout the whole temperature range studied, with a slight increase in *C* below T_m (Fig. 4 *A*). At T_m a local minimum is observed whereas further increase in temperature causes a small increment in *C*.

DNPC matrix

The influence of diBrChol on the temperature dependency of I_e/I_m of PyrPC was very similar to that observed for NBDchol with lower I_e/I_m ratios measured (not shown). Throughout the studied temperature range an efficient colocalization of PyrPC with diBrChol is observed (Fig. 4 *B*). In brief, when $T < T_m$ a small increase in *C* (enhanced close range colocalization) is evident. At ~2° below T_m a sudden decrease in *C* is seen, with a minimum at ~T_m. Further increase in *T* does not influence *C*.

For PyrSM with diBrChol the I_e/I_m values are lower than for PyrPC (not shown). *C* versus (T–T_m) shows smaller *C* values for PyrSM/diBrChol/DNPC compared to PyrPC/diBrChol/DNPC mixtures (Fig. 4 *B*). In brief, below T_m a slight decrease in *C* is observed, followed by a minimum at T_m. At $T > T_m$ a further decrement in *C* is evident.

DISCUSSION

This study was undertaken to explore the putative specific interaction between sphingomyelin and cholesterol. Our approach relied on the comparison between pyrene-labeled derivatives of phosphatidylcholine and sphingomyelin, PyrPC and PyrSM, respectively. Although the bulky pyrene moiety can be expected to distort the characteristics of these probes compared to the natural lipids, we may nevertheless anticipate the extent and nature of the perturbation to be equal for both lipid analogs. Furthermore, the pyrene moiety resides at the end of a 10-carbon atom spacer in both. Studies on the effects of cholesterol on phospholipids have revealed an increase in acyl chain order for carbon atoms 1–7, whereas a decrease in the order parameter was evident for the carbon atoms >7 (Rog and Pasenkiewicz-Gierula, 2001). This means that the membrane free volume distribution changes in the bilayer, increasing in the center in the presence of cholesterol. As the pyrene moiety is linked via a decanoyl chain, this causes the fluorophore to reside on the average deep in the bilayer. Accordingly, we may expect the pyrene moiety not to perturb the interactions between the planar sterol ring structure and the phospholipid acyl chain segments. Lastly, like for saturated phospholipids the calorimetric transition temperatures T_m for PyrSM and PyrPC used in this study are 43 and 15°C, respectively. In the light of the above we do consider it to be very unlikely that the presence of pyrene would fundamentally alter the behavior of the SM derivative, in particular its interactions with cholesterol.

Pyrene-labeled lipid derivatives have been extensively used in studies on biomembranes and their models (Lotta et al., 1988). Accordingly, their behavior is well documented

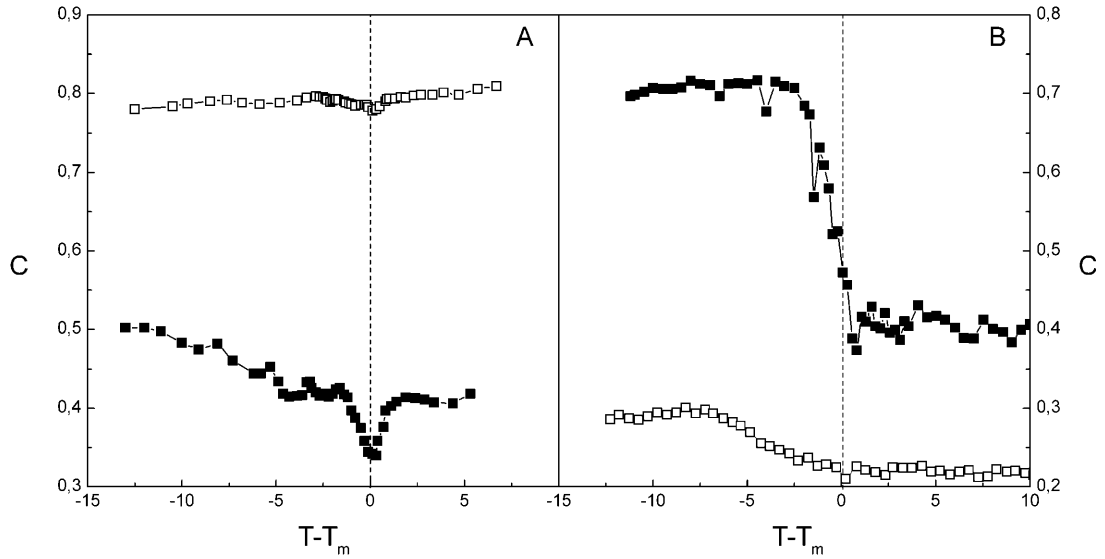

FIGURE 4 (*A*) Colocalization parameter *C* versus $T–T_m$ calculated for the PyrPC (■) or PyrSM (□) with 5,6-dibromo-cholestan-3β-ol collisional quencher pair in DMPC matrix. (*B*) Colocalization parameter *C* versus $T–T_m$ calculated for the PyrPC (■) or PyrSM (□) with 5,6-dibromo-cholestan-3β-ol collisional quencher pair residing in DNPC matrix. The experimental conditions were similar to those described in Fig. 1.

and understanding of the deviation of their properties from natural lipids can be exploited in the interpretation of the collected fluorescence data. PyrPC represents a substantial perturbing impurity to the packing of the DMPC and has been suggested to be distributed in a pseudohexagonal lattice to minimize the extent of perturbation (Somerharju et al., 1985; Virtanen et al., 1988; Tang and Chong, 1992). Partitioning of PyrPC into gel and fluid regions of DMPC should be approximately equal. Yet, upon increasing the temperature to T_0 PyrPC becomes transiently enriched in the formed fluid-in-gel domain boundaries (Jutila and Kinnunen, 1997), the sudden decrease in I_e/I_m just below T_m reflecting the disappearance of domain boundaries. Further increase in temperature ($T > T_m$) is likely to result in a uniform pseudohexagonal distribution of PyrPC (Somerharju et al., 1985). Below T_m of DMPC the sphingomyelin probe, PyrSM, forms clusters and prefers partitioning into the gel phase. Upon approaching T_m a decrease in I_e/I_m is observed and could reflect the disappearance of the gel phase and redistribution and dispersion of PyrSM molecules into the fluid matrix. Above T_m PyrSM is likely to be arranged into a pseudohexagonal lattice, similarly to PyrPC.

In the longer DNPC matrix PyrPC and PyrSM behave very differently. Both probes show a smooth and continuous behavior with I_e/I_m decreasing progressively upon $T \rightarrow T_m$. Notably, I_e/I_m values in the gel state DNPC are ~1 order-of-magnitude higher compared to DMPC. This is likely to result from the lack of constraints imposed by hydrophobic mismatch between the constituents (Lehtonen et al., 1996). In brief, the lengths of PyrPC and PyrSM exceed that of DMPC whereas both probes are significantly shorter than DNPC. The difference in I_e/I_m measured in the two matrices is likely to be due to interdigitation of the pyrene moieties into the hydrocarbon tails of the adjacent monolayer in DMPC, thus reducing collisional encounters required for the excimer formation. In keeping with the higher T_m for PyrSM than for PyrPC (43 versus 15°C) the chains of PyrSM should be more ordered and therefore the extent of interdigitation for PyrSM should exceed that for PyrPC. Accordingly, in DMPC the I_e/I_m values for PyrSM should be lower than for PyrPC, as observed. Approaching T_m of DNPC the dispersion of the clustered probes cause a sharp decrease in I_e/I_m. Above T_m of DNPC the values for I_e/I_m for both probes are nearly equal, yet slightly smaller for PyrSM.

After the characterization of the temperature-dependent fluorescence behavior of the two probes in DMPC and DNPC we proceeded to investigate the effects of cholesterol on I_e/I_m for the two probes both below and above the T_m of the matrices. As already outlined above specificity in the interaction of cholesterol and PyrSM over PyrPC could readily be anticipated to be reflected in I_e/I_m values. Moreover, the only perturbing factor is represented by the pyrene moiety and their perturbation can be expected to be relatively small, in addition to being identical for both probes. Accordingly, if cholesterol would preferentially interact with either PyrPC or PyrSM this should cause a more pronounced decrease in I_e/I_m for the probe preferred by cholesterol. The results show (Fig. 2) that cholesterol does not show any preferential interaction between PyrSM and the cholesterol derivatives either in DMPC or in fluid DNPC. In gel state DNPC we see pronounced and progressive decrement in I_e/I_m for both probes upon increasing cholesterol, in keeping with colocalization of cholesterol into the clusters enriched with the pyrene derivatives. We cannot exclude the possibility that the I_e/I_m would not detect small differences in the preference of interaction between cholesterol and PyrPC or PyrSM.

In a DMPC matrix and both in the presence as well as in the absence of the RET acceptor NBDchol the values of I_e/I_m are significantly lower for PyrSM than for PyrPC in the temperature range studied. In the gel phase (from 13 to 6°C below T_m), colocalization C of PyrPC and NBDchol decreases with temperature, whereas the opposite is observed for PyrSM (Fig. 3 *B*). The latter would be in keeping with the preferential partitioning of both PyrSM and NBDchol into the gel phase. Starting from T_0 both NBDchol and PyrPC enrich into the domain boundaries as shown by the increase in C (Jutila and Kinnunen, 1997). This is observed also for PyrSM and NBDchol. The maximum in C for PyrSM and NBDchol is observed at a slightly lower temperature than for PyrPC and NBDchol and could reflect a preference of PyrSM for the gel domains instead of the boundary (Veiga et al., 2001). At T_m minima are observed in I_e/I_m as well as C for both probes.

Distinctly from DMPC the I_e/I_m ratios for PyrSM and PyrPC show similar behavior in the presence of NBDchol both below and above the T_m of DNPC, contradicting a specific interaction between sphingomyelin and cholesterol. In brief, the presence of the RET acceptor should decrease I_e/I_m. In a DNPC matrix the opposite is observed, i.e., PyrPC appears to colocalize more efficiently with NBDchol than PyrSM (Fig. 3 *D*). The driving force for the colocalization of PyrSM with NBDchol in DMPC is likely to derive from the slightly longer hydrophobic thickness of PyrSM compared to PyrPC. Instead, in DNPC it is likely to be the chain-chain interactions of this matrix that will drive PyrPC to colocalize with cholesterol.

The RET results align with the data on collisional quenching of the pyrene-labeled lipids by diBrChol. In DMPC below T_m the values for C for PyrPC and diBrChol decreases. However, the sudden increase in C for PyrPC and NBDchol beginning at ~6° below T_m is not observed for diBrChol. This could imply that the peak in C at T^* reflects the properties of NBDchol. Due to the covalently linked fluorophore moiety NBDchol is significantly longer than diBrChol. The slight increase in C in at $T > T_m$ is likely to result from increased lateral mobility. The value for C measured for PyrSM/diBrChol in DMPC is much higher throughout the temperature range studied revealing co-enrichment of these probes, in contrast to PyrPC/diBrChol. Importantly, a small increase in C is observed below T_m supporting the RET data. At T_m a local minimum is observed followed by a slight increase in C above T_m. Taken together, the data for PyrSM and diBrChol are consistent with the PyrSM/NBDchol RET data. In DNPC matrix the opposite is observed, namely efficient colocalization of PyrPC with diBrChol and weaker colocalization of PyrSM with diBrChol, in perfect agreement with NBDchol RET data measured in this matrix. Lastly, it should be emphasized that both the RET studies and the collisional quenching data also included perturbing moieties in the cholesterol. Accordingly, although the results are in good agreement with the I_e/I_m results on the impact of cholesterol on PyrPC and PyrSM, it must be stressed that the presence of the NBD moiety and the iodines in cholesterol could sterically impair the interactions of this sterol with lipids compared to natural cholesterol.

The above results indicate a lack of a specific interaction between sphingomyelin and cholesterol and that the observed colocalization of cholesterol with either PyrPC or PyrSM in a DMPC matrix is likely to be explained by the hydrophobic mismatch of the constituents. This also provides a rational explanation for the reciprocal regulation of sphingomyelin and cholesterol levels in cells (Bretscher and Munro, 1993). Most of the evidence for a sphingomyelin-cholesterol complex formation derives from the apparent condensation observed in monolayers. Yet, this condensation is observed not only for sphingomyelin and cholesterol but has also been reported for phosphatidylcholine and cholesterol (Smaby et al., 1994, 1997) as well as DMPC and ceramide (Holopainen et al., 2001). To this end, the packing of lipids is determined by their effective shapes (Israelachvili et al., 1980) and is related to the lateral pressure profile (Cantor, 1997), with steric repulsion between the headgroups and the acyl chains, the effective size of the latter being determined by configurational entropy. The effective size of the headgroups also contains contribution by their hydration shells (Lehtonen and Kinnunen, 1995). Comparison of the compression isotherms for sphingomyelin and ceramide (the latter lacking the phosphocholine headgroup) reveals that a considerable fraction of the area occupied by sphingomyelin, ~8 Å^2 at 30 mN/m for *n*-palmitoyl-sphingomyelin (Holopainen et al., 2001), is due to the phosphocholine headgroup residing in the interface. This means that the weakly hydrated cholesterol can be partly accommodated underneath the headgroup, thus causing an apparent condensation in the compression isotherms. This conclusion was reached in recent Monte Carlo simulations of cholesterol-phospholipid mixtures showing that exposure of weakly hydrated cholesterol to water is energetically unfavorable and necessitates the formation of hydration shield by the strongly hydrated phosphocholine headgroup (Huang and Feigenson, 1999; Huang, 2002). Furthermore, the apparent condensation also has an apparent stoichiometry, determined by the sums of the molecular geometries and respective projections of surface areas. Due to the chain ordering effect of cholesterol the actual measured condensation is enhanced. Similar considerations apply to mixed monolayers of phosphatidylcholines and cholesterol (Smaby et al., 1994). The other line of evidence for sphingomyelin-cholesterol complex formation derives from the variation of rates of scavenging cholesterol from sphingomyelin/cholesterol monolayers by cyclodextrin into the subphase. Also in this system steric shielding of cholesterol by sphingomyelin headgroup together with the augmented van der Waals interactions between SM and cholesterol would readily explain the slower absorption rates at sphingomyelin/cholesterol stoichiometry <2:1 (Ohvo and Slotte, 1996). To this end, steric shielding of cholesterol by the phospholipid headgroups was suggested by

Barenholz and co-workers, studying the action of cholesterol oxidase on monolayers (Patzer et al., 1978). Lastly, the formation of the putative liquid-ordered domains constituted by sphingomyelin and cholesterol in a liquid-disordered membrane composed of unsaturated phosphatidylcholine, driven by hydrophobic mismatch, can be regarded as somewhat analogous to the formation of micelles, albeit in a two-dimensional system. Their organization is thus highly dynamic and the segregated liquid-ordered domains should be at rapid equilibrium with monomeric sphingolipid and cholesterol dissolved in the bulk phosphatidylcholine, with rapid exchange between the two phases.

We thank Drs. Tim Söderlund and Juha-Matti Alakoskela for critical reading of the manuscript.

Grants from the Paulo Research Foundation, Emil Aaltonen Foundation, Magnus Ehrnrooth Foundation (J.M.H.), and the Finnish Cultural Foundation (J.M.H. and A.J.) are acknowledged. MEMPHYS is supported by the Danish National Research Foundation and the Helsinki Biophysics & Biomembrane Group is supported by the Finnish Academy.

REFERENCES

Asturias, F. J., D. Pascolini, and J. K. Blasie. 1990. Evidence that lipid lateral phase separation induces functionally significant structural changes in the Ca^{2+}-ATPase of the sarcoplasmic reticulum. *Biophys. J.*58:205–217.

Bittman, R., C. R. Kasireddy, P. Mattjus, and J. P. Slotte. 1994. Interaction of cholesterol with sphingomyelin monolayers and vesicles. *Biochemistry.* 33:11776–11781.

Boggs, J. M. 1987. Lipid intermolecular hydrogen bonding: influence on structural organization and membrane function. *Biochim. Biophys. Acta.* 906:353–404.

Bretscher, M. S., and S. Munro. 1993. Cholesterol and the Golgi apparatus. *Science.* 261:1280–1281.

Brown, R. E. 1998. Sphingolipid organization in biomembranes: what physical studies of model membranes reveal. *J. Cell Sci.* 111:1–9.

Brown, D. A., and E. London. 2000. Structure and function of sphingolipid- and cholesterol-rich membrane rafts. *J. Biol. Chem.* 275:17221–17224.

Calhoun, W. I., and G. G. Shipley. 1979. Sphingomyelin-lecithin bilayers and their interaction with cholesterol. *Biochemistry.* 18:1717–1722.

Cantor, R. S. 1997. The lateral pressure profile in membranes: a physical mechanism of general anesthesia. *Biochemistry.* 36:2339–2344.

Curatolo, W. 1987. The physical properties of glycolipids. *Biochim. Biophys. Acta.* 906:111–136.

Demel, R. A., J. W. Jansen, P. W. van Dijck, and L. L. van Deenen. 1977. The preferential interaction of cholesterol with different classes of phospholipids. *Biochim. Biophys. Acta.* 465:1–10.

Drake, J. M., J. Klafter, and P. Levitz. 1991. Chemical and biological microstructures as probed by dynamic processes. *Science.* 251:1574–1579.

Estep, T. N., D. B. Mountcastle, Y. Barenholz, R. L. Biltonen, and T. E. Thompson. 1979. Thermal behavior of synthetic sphingomyelin-cholesterol dispersions. *Biochemistry.* 18:2112–2117.

Gatt, S., and E. L. Bierman. 1980. Sphingomyelin suppresses the binding and utilization of low density lipoproteins by skin fibroblasts. *J. Biol. Chem.* 255:3371–3376.

Guo, W., V. Kurze, T. Huber, N. H. Afdhal, K. Beyer, and J. A. Hamilton. 2002. A solid-state NMR study of phospholipid-cholesterol interactions: sphingomyelin-cholesterol binary systems. *Biophys. J.* 83:1465–1478.

Gupta, A. K., and H. Rudney. 1991. Plasma membrane sphingomyelin and the regulation of HMG-CoA reductase activity and cholesterol biosynthesis in cell cultures. *J. Lipid Res.* 32:125–136.

Glaser, M. 1995. Lipid domains in biological membranes. *Curr. Opin. Struct. Biol.* 3:475–481.

Holopainen, J. M., H. L. Brockman, R. E. Brown, and P. K. J. Kinnunen. 2001. Interfacial interactions of ceramide with dimyristoylphosphatidylcholine: impact of the *n*-acyl chain. *Biophys. J.* 80:765–775.

Hønger, T., K. Jørgensen, D. Stokes, R. L. Biltonen, and O. G. Mouritsen. 1997. Phospholipase A_2 activity and physical properties of lipid-bilayer substrates. *Methods Enzymol.* 286:168–190.

Hresko, R. C., I. P. Sugar, Y. Barenholz, and T. E. Thompson. 1986. Lateral distribution of a pyrene-labeled phosphatidylcholine in phosphatidylcholine bilayers: fluorescence phase and modulation study. *Biochemistry.* 25:3813–3823.

Hresko, R. C., I. P. Sugar, Y. Barenholz, and T. E. Thompson. 1987. The lateral distribution of pyrene-labeled sphingomyelin and glucosylceramide in phosphatidylcholine bilayers. *Biophys. J.* 51:725–735.

Huang, J. 2002. Exploration of molecular interactions in cholesterol superlattices: effect of multibody interactions. *Biophys. J.* 83:1014–1025.

Huang, J., and G. W. Feigenson. 1999. A microscopic interaction model of maximum solubility of cholesterol in lipid bilayers. *Biophys. J.* 76:2142–2157.

Hwang, J., L. A. Gheber, L. Margolis, and M. Edidin. 1998. Domains in cell plasma membranes investigated by near-field scanning optical microscopy. *Biophys. J.* 74:2184–2190.

Hwang, J., L. K. Tamm, C. Böhm, T. S. Ramalingam, E. Betzig, and M. Edidin. 1995. Nanoscale complexity of phospholipid monolayers investigated by near-field scanning optical microscopy. *Science.* 270:610–614.

Israelachvili, J. N., S. Marcelja, and R. G. Horn. 1980. Physical principles of membrane organization. *Q. Rev. Biophys.* 13:121–200.

Jacobson, K., E. D. Sheets, and R. Simson. 1995. Revisiting the fluid mosaic model of membranes. *Science.* 268:1441–1442.

Jutila, A., and P. K. J. Kinnunen. 1997. Novel features of the main transition of dimyristoylphosphocholine bilayers revealed by fluorescence spectroscopy. *J. Phys. Chem. B.* 101:7635–7640.

Keller, S. L., A. Radhakrishnan, and H. M. McConnell. 2000. Saturated phospholipids with high melting temperatures form complexes with cholesterol in monolayers. *J. Phys. Chem. B.* 104:7522–7527.

Kinnunen, P. K. J. 1991. On the principles of functional ordering in biological membranes. *Chem. Phys. Lipids.* 57:375–399.

Kolesnick, R. N. 1991. Sphingomyelin and derivatives as cellular signals. *Prog. Lipid Res.* 30:1–38.

Lakowicz, J. R. 1999. Quenching of fluorescence. *In* Principles of Fluorescence Spectroscopy, 2nd ed. J. R. Lakowicz, editor. Kluwer Academic/Plenum Publishers, New York. 237–289.

Lange, Y., J. S. D'Alessandro, and D. M. Small. 1979. The affinity of cholesterol for phosphatidylcholine and sphingomyelin. *Biochim. Biophys. Acta.* 556:388–398.

Lehtonen, J. Y. A., J. M. Holopainen, and P. K. J. Kinnunen. 1996. Evidence for the formation of microdomains in liquid crystalline large unilamellar vesicles caused by hydrophobic mismatch of the constituent phospholipids. *Biophys. J.* 70:1753–1760.

Lehtonen, J. Y. A., and P. K. J. Kinnunen. 1995. Poly(ethylene glycol)-induced and temperature-dependent phase separation in fluid binary phospholipid membranes. *Biophys. J.* 68:525–535.

Lehtonen, J. Y. A., and P. K. J. Kinnunen. 1997. Evidence for phospholipid microdomain formation in liquid crystalline liposomes reconstituted with *Escherichia coli* lactose permease. *Biophys. J.* 72:1247–1257.

Li, X.-M., M. M. Momsen, J. M. Smaby, H. L. Brockman, and R. E. Brown. 2001. Cholesterol decreases the interfacial elasticity and detergent solubility of sphingomyelins. *Biochemistry.* 40:5954–5963.

Lotta, T. I., L. J. Laakkonen, J. A. Virtanen, and P. K. J. Kinnunen. 1988. Characterization of Langmuir-Blodgett films of 1,2-dipalmitoyl-*sn*-

glycero-3-phosphatidylcholine and 1-palmitoyl-2-[10-(pyren-1-yl)decanoyl]-*sn*-glycero-3-phosphat idylcholine by FTIR-ATR. *Chem. Phys. Lipids*. 46:1–12.

Lund-Katz, S., H. M. Laboda, L. R. McLean, and M. C. Phillips. 1988. Influence of molecular packing and phospholipid type on rates of cholesterol exchange. *Biochemistry*. 27:3416–3423.

Mannock, D. A., T. J. McIntosh, X. Jiang, D. F. Covey, and R. N. McElhaney. 2003. Effects of natural and enantiomeric cholesterol on the thermotropic phase behavior and structure of egg sphingomyelin bilayer membranes. *Biophys. J*. 84:1038–1046.

Mattjus, P., and J. P. Slotte. 1996. Does cholesterol discriminate between sphingomyelin and phosphatidylcholine in mixed monolayers containing both phospholipids? *Chem. Phys. Lipids*. 81:61–80.

McConnell, H. M. 1991. Structures and transitions in lipid monolayers at the air-water interface. *Annu. Rev. Phys. Chem*. 42:171–195.

McIntosh, T. J., S. A. Simon, D. Needham, and C. H. Huang. 1992. Structure and cohesive properties of sphingomyelin/cholesterol bilayers. *Biochemistry*. 31:2012–2020.

Metso, A. J., A. Jutila, J.-P. Mattila, J. M. Holopainen, and P. K. J. Kinnunen. 2003. Nature of the main transition of dipalmitoylphosphocholine bilayers inferred from fluorescence spectroscopy. *J. Phys. Chem. B*. 107:1251–1257.

Mouritsen, O. G. 1998. Self-assembly and organization of lipid-protein membranes. *Curr. Opin. Coll. Interf. Sci*. 3:78–87.

Mouritsen, O. G., and M. Bloom. 1984. Mattress model of lipid-protein interactions in membranes. *Biophys. J*. 46:141–153.

Mouritsen, O. G., K. Jørgensen, and T. Hønger. 1995. Permeability of lipid bilayers near the phase transition. *In* Permeability and Stability of Lipid Bilayers. E. A. Disalvo and S. A. Simon, editors. CRC Press, Boca Raton, FL. 89–112.

Mouritsen, O. G., and P. K. J. Kinnunen. 1996. Role of lipid organization and dynamics for membrane functionality. *In* Biological Membranes. K. Merz, Jr., and B. Roux, editors. Birkhäuser, Boston, MA. 463–502.

Mustonen, P., J. A. Virtanen, P. J. Somerharju, and P. K. J. Kinnunen. 1987. Binding of cytochrome c to liposomes as revealed by the quenching of fluorescence from pyrene-labeled phospholipids. *Biochemistry*. 26:2991–2997.

Needham, D., and R. S. Nunn. 1990. Elastic deformation and failure of lipid bilayer membranes containing cholesterol. *Biophys. J*. 58:997–1009.

Ohvo, H., L. Olsio, and J. P. Slotte. 1997. Effects of sphingomyelin and phosphatidylcholine degradation on cyclodextrin-mediated cholesterol efflux in cultured fibroblast. *Biochim. Biophys. Acta*. 1349:131–141.

Ohvo, H., and J. P. Slotte. 1996. Cyclodextrin-mediated removal of sterols from monolayers: effects of sterol structure and phospholipids on desorption rate. *Biochemistry*. 35:8018–8024.

Okwu, A. K., X. X. Xu, Y. Shiratori, and I. Tabas. 1994. Regulation of the threshold for lipoprotein-induced acylCoA:cholesterol O-acyltransferase stimulation in macrophages by cellular sphingomyelin content. *J. Lipid Res*. 35:644–655.

Patzer, E. J., R. R. Wagner, and Y. Barenholz. 1978. Cholesterol oxidase as a probe for studying membrane organisation. *Nature*. 274:394–395.

Pörn, M. I., M. P. Ares, and J. P. Slotte. 1993. Degradation of plasma membrane phosphatidylcholine appears not to affect the cellular cholesterol distribution. *J. Lipid Res*. 34:1385–1392.

Radhakrishnan, A., R. G. Anderson, and H. M. McConnell. 2000. Condensed complexes, rafts, and the chemical activity of cholesterol in membranes. *Proc. Natl. Acad. Sci. USA*. 97:12422–12427.

Radhakrishnan, A., X.-M. Li, R. E. Brown, and H. M. McConnell. 2001. Stoichiometry of cholesterol-sphingomyelin condensed complexes in monolayers. *Biochim. Biophys. Acta*. 1511:1–6.

Ramstedt, B., and J. P. Slotte. 1999. Interaction of cholesterol with sphingomyelins and acyl-chain-matched phosphatidylcholines: a comparative study of the effect of the chain length. *Biophys. J*. 76:908–915.

Rog, T., and M. Pasenkiewicz-Gierula. 2001. Cholesterol effects on the phosphatidylcholine bilayer nonpolar region: a molecular simulation study. *Biophys. J*. 81:2190–2202.

Sankaram, M. B., and T. E. Thompson. 1990. Interactions of cholesterol with various glycerophospholipids and sphingomyelin. *Biochemistry*. 29:10670–10675.

Sankaram, M. B., and T. E. Thompson. 1991. Cholesterol-induced fluid-phase immiscibility in membranes. *Proc. Natl. Acad. Sci. USA*. 88:8686–8690.

Schroeder, F., and G. Nemecz. 1989. Interaction of sphingomyelins and phosphatidylcholines with fluorescent dehydroergosterol. *Biochemistry*. 28:5992–6000.

Slotte, J. P., 1999. Sphingomyelin-cholesterol interactions in biological and model membranes. *Chem. Phys. Lipids*. 102:13–27.

Slotte, J. P., and E. L. Bierman. 1988. Depletion of plasma-membrane sphingomyelin rapidly alters the distribution of cholesterol between plasma membrane and intracellular cholesterol pools in cultured fibroblasts. *Biochem. J*. 250:653–658.

Smaby, J. M., H. L. Brockman, and R. E. Brown. 1994. Cholesterol's interfacial interactions with sphingomyelins and phosphatidylcholines: hydrocarbon chain structure determines the magnitude of condensation. *Biochemistry*. 9:9135–9142.

Smaby, J. M., M. M. Momsen, H. L. Brockman, and R. E. Brown. 1997. Phosphatidylcholine acyl unsaturation modulates the decrease in interfacial elasticity induced by cholesterol. *Biophys. J*. 73:1492–1505.

Somerharju, P. J., J. A. Virtanen, K. K. Eklund, and P. K. J. Kinnunen. 1985. 1-Palmitoyl-2-pyrenedecanoyl glycerophospholipids as membrane probes: evidence for regular distribution in liquid-crystalline phosphatidylcholine bilayers. *Biochemistry*. 24:2773–2781.

Streitwieser, A., Jr., and C. H. Heathcock. 1985. Electrophilic aromatic substitution. *In* Introduction to Organic Chemistry, 3rd Ed. Macmillan Publishing Company, New York. 645–680.

Tang, D., and P. L.-G. Chong.1992. Evidence for lipids regularly distributed into hexagonal super-lattices in pyrene-PC/DMPC binary mixtures at specific concentrations. *Biophys. J*. 63:903–910.

Untracht, S. H., and G. G. Shipley. 1977. Molecular interactions between lecithin and sphingomyelin. Temperature- and composition-dependent phase separation. *J. Biol. Chem*. 252:4449–4457.

Varma, R., and S. Mayor. 1998. GPI-anchored proteins are organized in submicron domains at the cell surface. *Nature*. 394:798–801.

Vaz, W. L. C., and P. F. F. Almeida. 1993. Phase topology and percolation in multi-phase lipid bilayers: is the biological membrane a domain mosaic? *Curr. Opin. Struct. Biol*. 3:482–488.

Veiga, M. P., J. L. R. Arrondo, F. M. Gõni, A. Alonso, and D. Marsh. 2001. Interaction of cholesterol with sphingomyelin in mixed membranes containing phosphatidylcholine, studied by spin-label ESR and IR spectroscopies. A possible stabilization of gel-phase sphingolipid domains by cholesterol. *Biochemistry*. 40:2614–2622.

Virtanen, J. A., P. Somerharju, and P. K. J. Kinnunen. 1988. Prediction of patterns for the regular distribution of soluted guest molecules in liquid crystalline phospholipid membranes. *J. Mol. Electr*. 4:233–236.

Weis, R. M., and H. M. McConnell. 1985. Cholesterol stabilizes the crystal-liquid interface in phospholipid monolayers. *J. Phys. Chem*. 89:4453–4459.